Geophysical Research Letters

RESEARCH LETTER
10.1029/2026GL122196

The Role of Link Length Hierarchy on Dynamic Connectivity in River Networks Across Climatic Regimes

Dnyanesh Borse[1], Juthika Roy[1], Alejandro Tejedor[2,3,4], Efi Foufoula-Georgiou[4], and Arvind Singh[1]

[1]Department of Civil, Environmental, and Construction Engineering, University of Central Florida, Orlando, FL, USA, [2]Institute for Biocomputation and Physics of Complex Systems (BIFI), University of Zaragoza, Zaragoza, Spain, [3]Department of Theoretical Physics, University of Zaragoza, Zaragoza, Spain, [4]Department of Civil and Environmental Engineering, University of California, Irvine, CA, USA

Key Points:

- We quantify how the spatial organization of channel lengths control the convergence of fluxes across river networks
- Link-length hierarchy across stream orders controls minimal flow connectivity, while side-branching controls maximal flow connectivity
- Humid basins characterized by a stronger link-length hierarchy and greater side-branching exhibit slower flux aggregation than dry basins

Supporting Information:

Supporting Information may be found in the online version of this article.

Correspondence to:

A. Singh and A. Tejedor,
arvind.singh@ucf.edu;
atejedor@unizar.es

Citation:

Borse, D., Roy, J., Tejedor, A., Foufoula-Georgiou, E., & Singh, A. (2026). The role of link length hierarchy on dynamic connectivity in river networks across climatic regimes. *Geophysical Research Letters*, *53*, e2026GL122196. https://doi.org/10.1029/2026GL122196

Received 1 FEB 2026
Accepted 7 MAY 2026

Author Contributions:

Conceptualization: Alejandro Tejedor, Efi Foufoula-Georgiou, Arvind Singh
Formal analysis: Dnyanesh Borse
Funding acquisition: Arvind Singh
Investigation: Dnyanesh Borse
Methodology: Dnyanesh Borse, Juthika Roy, Alejandro Tejedor, Arvind Singh
Project administration: Arvind Singh
Software: Dnyanesh Borse, Juthika Roy, Alejandro Tejedor
Supervision: Efi Foufoula-Georgiou, Arvind Singh
Visualization: Dnyanesh Borse

Abstract Connectivity within river networks governs the transport and aggregation of fluxes such as water, sediment, and nutrients. Here we focus on *dynamic connectivity* (*DC*), defined by the time-evolving connectivity that emerges as fluxes propagate and mix through the network, characterized by minimal-flow connectivity (DC_{min}) and maximal-flow connectivity (DC_{max}). Using 100 natural basins across the United States, we disentangle the roles of network geometry (link-lengths) and topology (branching structure) in controlling the times to achieve DC_{min} and DC_{max}. We find that link-lengths decrease with stream order, and this geometric hierarchy primarily controls the time to DC_{min}, whereas the time to DC_{max} is mainly governed by network topology. Placed in a climatic context, our results show that humid basins, characterized by stronger link-length hierarchy and enhanced side branching, exhibit slower flux aggregation. This study provides new insights into how climate influences channel network geometry and topology, thereby controlling basin-scale flux aggregation rates.

Plain Language Summary River networks act as nature's drainage systems, moving water, sediment, and nutrients from the landscape to the ocean or water bodies. How quickly these fluxes connect and mix throughout a basin depends on both the structural arrangement of channels (topology) and their size (geometry) within the river network. In this study, we use a dynamic connectivity framework to track how fluxes from different parts of a river network aggregate over time. We find that the arrangement and length of river links strongly influence this process: when higher-order links are relatively shorter than the lower-order links, that is, more hierarchically arranged, it takes longer for fluxes to start mixing, whereas networks with more side-branches delay the travel for all fluxes to converge at the outlet. Comparing basins across different climates, we show that humid basins, which tend to have more side-branches and more hierarchical link lengths, exhibit slower dynamic connectivity than basins in dry regions. This slower dynamic connectivity allows humid basins to naturally attenuate and disperse flood peaks, suggesting that this emergent property may be a fundamental driver of the networks' topological and geometric evolution.

1. Introduction

Connectivity within river networks governs how environmental fluxes such as water, sediment, and nutrients are transported across landscapes (Benda et al., 2004; Cushman & McGarigal, 2002; Hansen & Singh, 2018; Rodriguez-Iturbe & Rinaldo, 1997). River networks also serve as ecological corridors that regulate the movement and dispersal of organisms through hydrologic connectivity, nutrient cycling, and habitat connectivity across spatial and temporal scales (Bracken & Croke, 2007; Carrara et al., 2012; Larsen et al., 2012; Muneepeerakul et al., 2008; Rinaldo et al., 2020; Rodriguez-Iturbe et al., 2009; Wohl et al., 2019). From a geomorphological perspective, the patterns of network connectivity also determine the pathways of energy and material transfer that shape landscape evolution and determine the efficiency of environmental transport (Carraro et al., 2020; Rodriguez-Iturbe & Rinaldo, 1997). Therefore, understanding the spatial structure of river networks (e.g., arrangement of channels) as well as the temporal evolution of patterns of fluxes propagating on those networks is essential for quantifying processes ranging from flood generation and sediment routing to the persistence and evolution of aquatic populations (Botter et al., 2011; Carrara et al., 2014; Czuba & Foufoula-Georgiou, 2014; Garbin et al., 2019; Kiffney et al., 2006; Shao et al., 2019; Zaliapin et al., 2010).

Writing – original draft: Dnyanesh Borse, Alejandro Tejedor, Arvind Singh
Writing – review & editing: Dnyanesh Borse, Alejandro Tejedor, Arvind Singh

Several metrics have been proposed to quantify structural connectivity in river networks, spanning geometric, graph-theoretic, and hydrologic perspectives. Structural indices such as drainage density, junction angle, and bifurcation ratio characterize the spatial organization of channels (Coffey & Shaw, 2017; Hooshyar et al., 2017; Horton, 1945; Kovchegov et al., 2022b; Ranjbar et al., 2018; Rodriguez-Iturbe & Rinaldo, 1997; Sassolas-Serrayet et al., 2018; Schumm, 1956; Seybold et al., 2017). Early hydrologic frameworks further linked drainage network structure to basin-scale response through concepts such as width functions and unit hydrographs, enabling spatio-temporal analysis of runoff routing and system response (Gupta et al., 1980; Kirkby, 1976; Rodríguez-Iturbe & Valdés, 1979; Troutman & Karlinger, 1985). Graph-based approaches further quantify properties such as path lengths, branching asymmetry, and critical nodes that govern flux transfer and fragmentation (Carrara et al., 2012; Kovchegov et al., 2022a; Sarker et al., 2019, 2025; Tejedor et al., 2015; Zanardo et al., 2013). More recently, hydrologic connectivity metrics have incorporated the temporal activation of flow paths to assess how fluxes propagate under varying climatic or event conditions (Botter et al., 2021; Bracken & Croke, 2007; Garbin et al., 2019). Yet despite this progress, most existing frameworks treat connectivity as a static attribute, leaving its time-evolving behavior during flux propagation largely unexamined.

While static network representations capture the overall channel arrangement, the temporal dynamics of connectivity, that is, how and when different parts of the network become hydrologically or ecologically connected, are equally crucial (Rinaldo et al., 2020). Recent work by Roy et al. (2022) introduced a dynamic connectivity framework that captures the evolution of flux aggregation processes through the formation of time-dependent clusters. Within that framework, a river network achieves minimal dynamic connectivity ($DC_{\min}$), when fluxes from at least two upstream sources have reached every point in the river network, resulting in minimum mixing. The minimal dynamic connectivity controls the spread of ecological communities and pollutants (Botter et al., 2021; Garbin et al., 2019). On the other hand, the river network attains maximal (i.e., peak-flow) dynamic connectivity ($DC_{\max}$), when at any point on the network, the fluxes from all upstream sources are mixed. This condition implies that the source located farthest from the outlet has contributed to the flow at the outlet. This connectivity, based on the full aggregation, reflects the basin-scale transport efficiency, sediment delivery, and the timing and magnitude of hydrograph peaks. Together, these two connectivity criteria describe the temporal evolution of network activation, from the initiation of connected flow paths to the complete aggregation of fluxes, and are central to understanding how basins respond to climatic and hydrologic forcing.

Importantly, dynamic connectivity is inherently constrained by the (static) structural properties of the river network through which fluxes propagate. For example, the topology of river networks, defined as the connection between the junctions and channels of the network, plays a key role in governing the timing and rate of dynamic connectivity, with the abundance of side-branching (i.e., merging of channels of different orders) junctions acting as a topological brake that slows the propagation of fluxes (Roy et al., 2022). However, the influence of geometry (e.g., channel length) has remained largely unexplored. Moreover, the combined effects of topology and geometry, and their dependence on climatic conditions, are poorly understood. Observations suggest that humid basins exhibit more side-branching and different link-length distributions than arid basins (Dodds & Rothman, 2000; Ranjbar et al., 2018; Yang & Lee, 2001; Zanardo et al., 2013), yet the mechanistic basis by which these structural attributes influence dynamic connectivity and flood response remains unresolved.

Here, we develop a generalized dynamic connectivity framework to explicitly disentangle the roles of topology and geometry in governing the temporal evolution of flux aggregation. We investigate how climatic variability influences the connectivity across natural basins given the variations in branching configuration and link-length distributions.

2. Methods and Data Analyzed

2.1. Dynamic Connectivity Framework

In this study, we employ the dynamic connectivity framework introduced by Roy et al. (2022) (see also Zaliapin et al. (2010); Kovchegov et al. (2023); Duquesne and Winkel (2019)), which captures the emergent connectivity—via dynamic clusters—that arises from the transport of fluxes through the static river network structure. A dynamic cluster is defined as a set of nodes or links (here river-network's junctions or channels) that become connected through the downstream propagation of fluxes at a given time. We define clusters according to two alternative criteria which are relevant to different eco-hydro-geomorphological processes: (a) minimum flow conditions: a catchment (or a part of a catchment) is defined as a cluster if all their channels and junctions receive

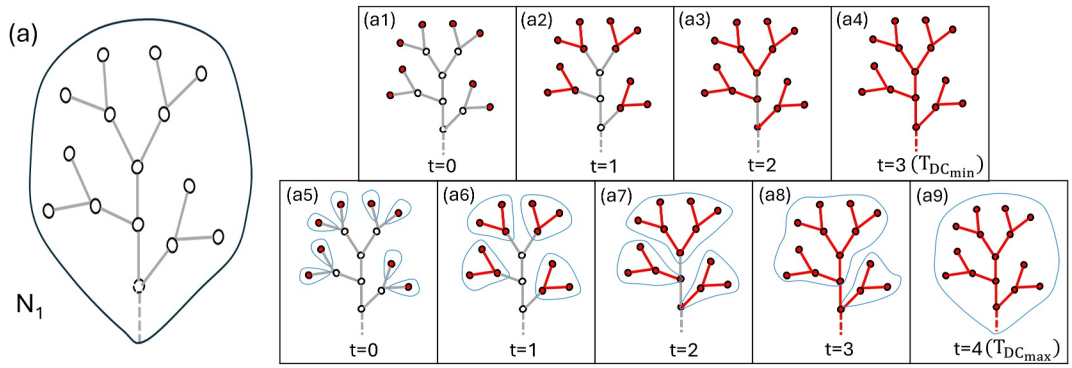

Figure 1. (a) A sample river network (N_1) with constant link lengths representing network topology. In response to a constant flux input imposed at time $t = 0$ to all source nodes and assuming same flux propagation rate in all links, panels (a1)–(a4) show the steps of dynamic connectivity forming distinct clusters of connected links based on minimal dynamic connectivity ($DC_{\min}$), that is, when fluxes from at least two upstream sources are mixed. Panels (a5)–(a9) show steps of dynamic connectivity based on maximal dynamic connectivity ($DC_{\max}$), that is, when fluxes from all source nodes are mixed. Note that in previous studies (Roy et al., 2022), minimum and maximum dynamic connectivity conditions have been referred to as structural and time-of-concentration, respectively.

fluxes from at least two upstream sources, achieving the $DC_{\min}$ condition; (b) peak- (maximum-) flow condition: a catchment is defined to be a cluster if all its constituent channels and junctions receive fluxes from all the upstream sources, achieving its $DC_{\max}$ condition. As the time progresses, the size (i.e., catchment extent) and number of clusters evolve. Thus, a full characterization of the dynamic connectivity of a river network includes the evolution of connectivity rather than just the static spatial connectivity of nodes and links across the landscape.

Figure 1 illustrates the evolution of clusters on a schematic river network when fluxes from all source nodes are injected at the same time (Figure 1a) and under the two above discussed dynamic connectivity scenarios, $DC_{\min}$ (Figures 1a1–1a4) and $DC_{\max}$ (Figures 1a5–1a9). The evolution is shown from $t = 0$ until basin-wide connectivity is achieved, at which point a single cluster spans the entire river network. We define $T_{DC_{\min}}$ as the time to basin-wide connectivity under $DC_{\min}$, that is, minimum mixing is guaranteed (at least two upstream sources contribute) across the whole river network's spatial extent (Figure 1a4). In contrast, basin-wide connectivity under $DC_{\max}$ is reached at time $T_{DC_{\max}}$, when all channels and junctions within the river network, including the outlet, receive contributions from all upstream sources (Figure 1a9).

The time required for a channel network to achieve minimum flow connectivity ($T_{DC_{\min}}$) and peak flow connectivity ($T_{DC_{\max}}$) depends on both topology (i.e., how channels are connected) and geometry (i.e., the variation in channel lengths). Roy et al. (2022) explicitly explored the effect of topology on dynamic connectivity. Here, we explore whether the link length distribution or their spatially heterogeneous arrangement exerts control on the emergent dynamic connectivity of river networks. To do so, we test the differences in this emergent dynamic connectivity for river networks that are topological twins of the observed networks, but with different geometric (link-length) scenarios. These scenarios include: one in which link lengths are forced to be uniform, one that preserves the observed length of every link, and one that preserves the link-length distribution while spatially reshuffling individual values.

2.2. Data Analyzed

We analyze 100 natural river basins across the United States with minimal human disturbance, representing diverse geographic and climatic regions. Among them, 50 basins are located in dry zones characterized by a higher aridity index AI (>3) and lower mean annual precipitation MAP (<700 mm yr^{-1}), while the remaining 50 basins belong to humid zones with lower AI (<3) and higher MAP (>1000 mm yr^{-1}). The geographical locations of these 100 basins are shown in Figure 2a and the distribution of basin sizes is shown in Figure S1a in Supporting Information S1. The selected basins span drainage areas from 0.4 to 20.5 km^2, AI values ranging from 0.32 to 45.7, and MAP from 71 to 2,797 mm yr^{-1}. Digital elevation data were obtained from the U.S. Geological Survey, and channel networks were extracted from 5 m resolution digital elevation models (DEMs) using a curvature-based method (see Hooshyar et al. (2016) and also Passalacqua et al. (2010)), which delineates valleys

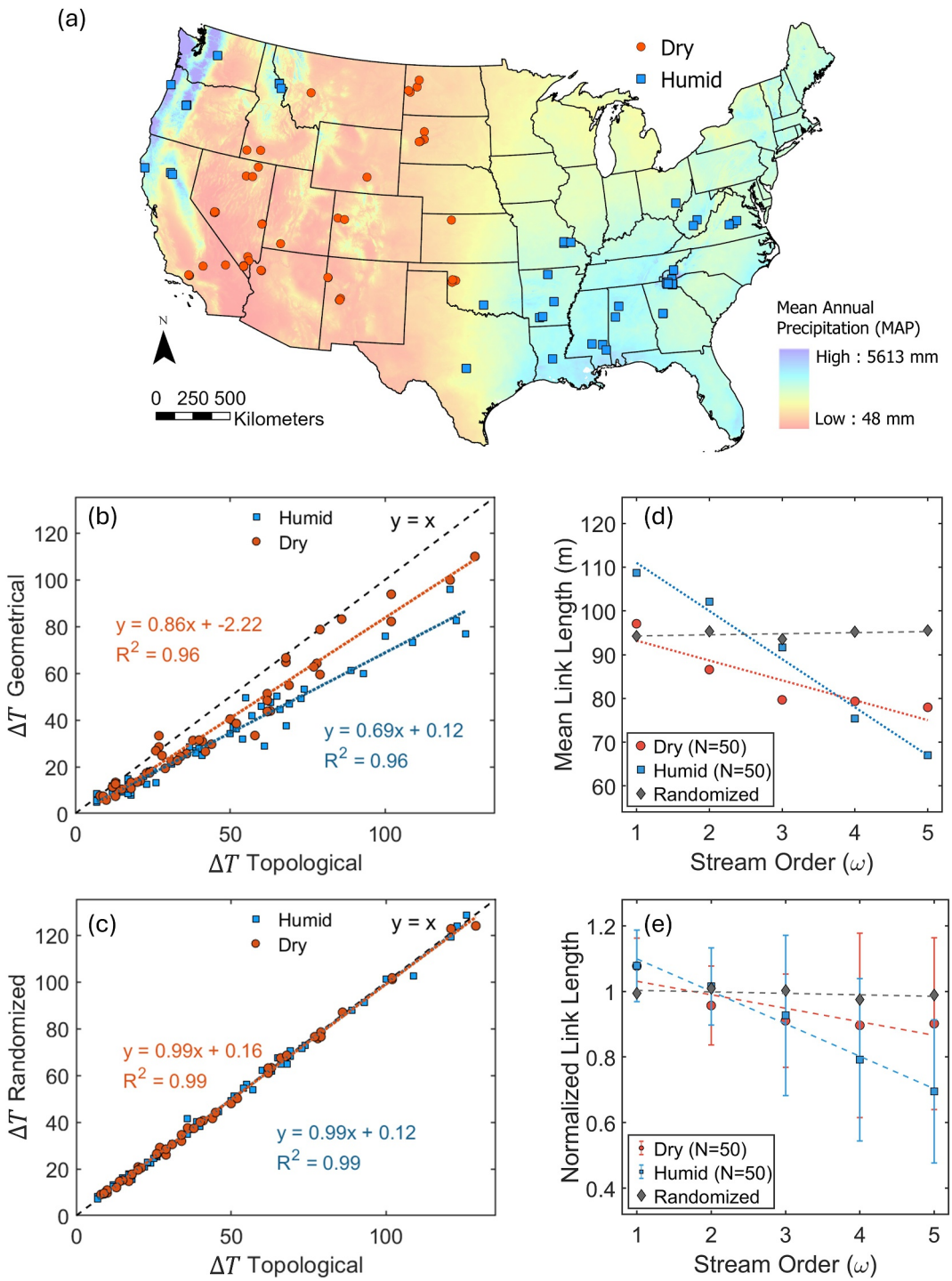

Figure 2. (a) The geographical locations of 100 natural basins analyzed from dry and humid climatic regions to study the effect of link length variability on mixing time ($\Delta T = DC_{\max} - DC_{\min}$) (b) ΔT geometrical (calculated based on actual link lengths normalized with respect to the mean link length of the corresponding basins) versus ΔT topological (assuming unit length for all links). (c) When link lengths are randomly shuffled with a fixed topological structure of the network, the ΔT_{Geom} falls onto ΔT_{Topo}, highlighting the clear effect of link length geometry on the overall network structure. (d) Variation of ensemble mean link lengths of 50 dry and 50 humid basins with respect to stream order. (e) Normalized link lengths (normalized with respect to the mean link length of that individual basin) for humid (blue color), dry (red color), and randomized condition (gray) as a function of stream order. Circle, square and diamond indicate overall mean of dry humid and randomized link lengths and error bars indicate ±1 standard error with respect to the mean. The difference in the hierarchy is visible in the ΔT_{Geom} (see b, c). When we randomly shuffle the link lengths for the same network topology, the hierarchy with respect to stream orders vanishes, as shown by the dashed line.

and channels based on local topographic curvature and k-means clustering of contour lines. We extracted the *AI* (defined here as the ratio of mean annual potential evapotranspiration to precipitation) for basins from the global aridity index data set based on global climate data from 1970 to 2000 (Zomer et al., 2022), and *MAP* was extracted based on the 30-year (1990–2019) annual average of the precipitation data set for North America (Wieczorek & Signell, 2023).

The extracted channel networks provide spatial connections between all nodes and junctions, along with their corresponding link lengths. From these networks, we compute topological properties such as the degree of side-branching, quantified by the Tokunaga parameter (c-value), where a higher c-value indicates a greater abundance of side-tributaries (Peckham, 1995; Ranjbar et al., 2020; Tokunaga, 1978). For simplicity, we assume a constant flux velocity of 1 m/s to calculate the ($T_{DC_{\min}}$) and ($T_{DC_{\max}}$) thus rendering distance and time interchangeable. We also calculate $\Delta T\ (=T_{DC_{\max}} - T_{DC_{\min}})$ as a summary metric and use it to assess how the emergent overall dynamic connectivity at both minimal- and peak flow depends on geometrical and topological controls, as well as climatic conditions. Finally, to understand how river-network topology and geometry influence the system's overall dynamical response, we compute the rate of flux aggregation at the outlet, which is analogous to a hydrograph (Ghotbi et al., 2020; Gupta et al., 1980; Rodríguez-Iturbe & Valdés, 1979). We then compare how the aggregation rate evolves from flux initiation to basin-wide $DC_{\min}$ and $DC_{\max}$, across climatic regimes.

3. Results and Discussion

3.1. Dynamic Connectivity in Natural Basins and the Role of Hierarchical Link Lengths

Roy et al. (2022) demonstrated that dynamic connectivity depends on the topological properties of a river network, showing that when only topological variations are considered, networks with higher side-branching achieve $DC_{\min}$ earlier (i.e., smaller $T_{DC_{\min}}$) but require a larger $T_{DC_{\max}}$. In this work, we aim to demonstrate the role of geometry (link lengths) on the emergent dynamic connectivity.

To disentangle the influence of geometry from that of topology, we computed $T_{DC_{\min}}$, $T_{DC_{\max}}$, and their difference ΔT for each basin under two configurations: (a) the *geometrical case*, which incorporates the actual link lengths in the river network, and (b) the *topological case*, where all links were assigned a constant length equal to the basin's mean link-length.

Figure 2b shows that ΔT_{geom} is consistently smaller than ΔT_{topo} for all basins, indicating that the observed variability in link lengths induces an acceleration in the progression from $DC_{\min}$ to $DC_{\max}$. Moreover, humid basins display systematically lower ΔT values than dry basins, suggesting that differences in link-length organization contribute to the observed climatic contrast.

To determine whether the acceleration in dynamic connectivity is intrinsically driven by the variability in link length or whether it is grounded in the spatial heterogeneity of that variability, we perform a reshuffling experiment, where link lengths are randomized across the network structure, thereby removing preexisting spatial heterogeneity in link lengths across the preserved topology. The results of this experiment show that ΔT_{random} collapses onto ΔT_{topo} (Figure 2c). This convergence confirms that the reduced ΔT observed in the geometric case is driven by the spatial heterogeneity of link lengths and not due to its intrinsic variability.

To explore the nature of link-length heterogeneity, we analyzed the ensemble mean link-length as a function of stream order (see Figure 2d and Figure S2 in Supporting Information S1) for the 100 basins in this study, segregated into two groups according to whether they belong to humid or arid environments. Both humid and dry basins exhibit a hierarchical pattern in which link lengths decrease with stream order, with the hierarchy being more pronounced in humid basins. Similar trends are observed when link lengths are normalized (with respect to mean link length of individual basins) to account for variations in basin size (see Figure 2e). Note that in this study, we adopt the Horton–Strahler stream-order convention (Horton, 1945; Strahler, 1957). Thus, the observation that ΔT_{geom} is consistently smaller than ΔT_{topo} is due to the observed hierarchy in link-lengths (noting that an opposite hierarchical relation, where lower-order streams have shorter links than higher-order ones, would yield $\Delta T_{geom} > \Delta T_{topo}$, a behavior not observed in the analyzed natural basins). The existence of these order-based hierarchical patterns (see Figure 2d), and the differences between them, emerge as the primary driver of the distinct dynamic-connectivity responses shown in Figure 2b, an interpretation further supported by the disappearance of these differences when link-length values are spatially randomized as shown in Figure 2c. This

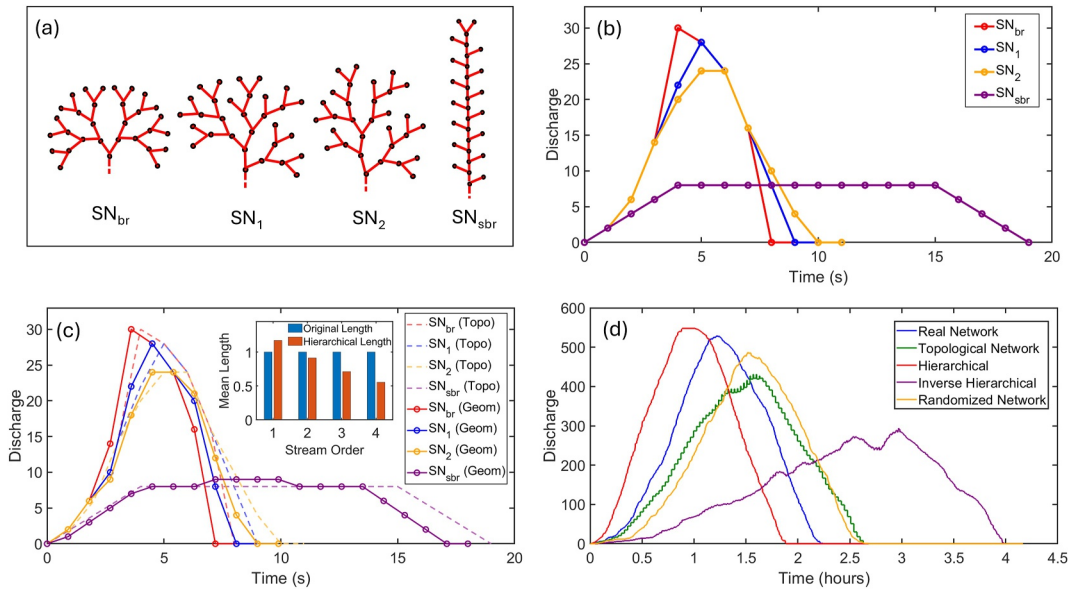

Figure 3. The effect of network topology and geometry on flux aggregation. (a) Schematic showing four synthetic networks with different topology. SN_{br} represents pure branching, SN_{sbr} represents maximum possible side-branching, SN_1 and SN_2 represent networks with increasing side-branching respectively. (b) Effect of pure topology (with all link lengths = 1) on flux aggregation. (c) By introducing hierarchy in link lengths while keeping the total link length constant, for example, as shown in the inset for the case of SN_{br}, we find that the total $DC_{\max}$ or time to maximal dynamic connectivity ($T_{DC_{\max}}$) reduces, that is, hydrograph shifts to the left. (d) Effect of link-length variation on hydrographs for a real river network. The natural hierarchical geometry produces the reference hydrograph (blue). Increasing geometric hierarchy shifts the hydrograph earlier (red), whereas removing hierarchy—by assigning equal link lengths (green) or randomly shuffling link lengths (yellow)—delays aggregation. Imposing an inverse hierarchy, in which higher-order channels have longer links, further delays aggregation. Such elongated configurations resemble networks with enhanced side branching (see SN_{sbr}).

observation further suggests that the hierarchy enhances the heterogeneity of the flux travel distances, promoting faster mixing and smaller ΔT_{geom}.

3.2. The Role of Topology and Geometry on the Rate of Flux Aggregation

The rate of flux aggregation through a river network at the outlet quantifies how quickly channels contribute their fluxes to the outlet over time. It is analogous to the temporal gradient (slope) of a hydrograph, which represents how discharge changes with time at a specific point in a basin's river network. Here, we compute this rate by tracking the number of nodes (or links) that become connected to the outlet as fluxes propagate downstream. For simplicity, we assume unit velocity of 1 m s^{-1} for flux propagation, allowing distance and time to be used interchangeably. This analysis provides direct insight into how network structure influences the timing and shape of the aggregation curve, which reflects the efficiency of flux convergence within the basin.

To gain insight into the relative roles of topology and geometry, we first examined four synthetic networks with distinct topological configurations, ranging from pure branching (i.e., merging of channels of the same order; SN_{br}) through increasing side-branching (SN_1 and SN_2) to the maximum possible side-branching structure (SN_{sbr}; Figure 3a). To isolate the effect of topology, all link lengths were assigned a uniform value of 1. The resulting hydrographs (Figure 3b), assuming a spatially uniform precipitation, reveal that a purely side-branching structure (SN_{sbr}) exhibits delayed and broader peak, indicating slower flux aggregation and a longer time to peak flow connectivity. In contrast, the purely branching configuration (SN_{br}) shows a sharper and earlier peak, reflecting faster flux convergence, while the two intermediate branching structures (SN_1 and SN_2) fall in between.

To explore the effect of geometry, we introduced a link-length hierarchy on the synthetic networks discussed above and shown in Figure 3a while keeping the total network length constant (see inset in Figure 3c). This inset illustrates the hierarchical variation of the link lengths for the sample network (SN_{br}), where lower-order links were assigned longer lengths relative to higher orders. The resulting hydrographs suggest that increasing geometric hierarchy shifts the time to peak aggregation earlier, reducing the overall $T_{DC_{\max}}$. This highlights that

geometric heterogeneity, characterized by introducing longer link lengths for numerous small tributaries and smaller link lengths for higher order links, facilitates faster connectivity even under an identical topology.

We also tested the influence of link-length hierarchy using a real network (Figure 3d). The hydrographs show that networks with a stronger (steeper decay of average link length with stream order) geometric hierarchy (red) exhibit earlier peaks compared to those with equal link lengths (green) or randomly shuffled lengths (yellow). The latter two, which lack an ordered hierarchy, display delayed and broader peaks consistent with slower flux aggregation. When an inverse hierarchy was imposed, where higher-order streams are longer than lower-order streams, the peak was further delayed, mimicking the behavior of side-branching networks (SN_{sbr}). Such inverse configurations are uncommon in nature but demonstrate how geometric elongation can emulate the hydrologic effect of increased side-branching. Overall, these results emphasize that topology primarily dictates the overall shape and timing of aggregation, whereas geometry modulates its rate and efficiency by controlling the hierarchical distribution of link lengths.

3.3. Climatic Influence on the Rate of Aggregation

To examine how climate influences the rate of flux aggregation, we compare aggregation rates between humid and dry basins. Humid basins exhibit greater side-branching, as reflected in higher Tokunaga c-values (see Figure S1 in Supporting Information S1 and also Zanardo et al. (2013); H. Bavojdan et al. (2025)). As discussed above, humid basins also exhibit a stronger link-length hierarchy (see Figure 2d and Figure S2 in Supporting Information S1). Here, we investigate how the combined effects of topology and geometry on flux aggregation manifest in the natural basins.

Figures 4a and 4b show two representative basins of similar drainage areas $(\sim 5\ \mathrm{km}^2)$ but significantly different aridity index (AI) and mean annual precipitation (MAP). The humid basin (AI = 0.7, MAP ~ 1,858 mm) exhibits higher side-branching (c-value = 2.7) and longer link lengths with a stronger link length hierarchy, whereas the dry basin (AI = 5.4, MAP ~ 352 mm) shows a more branched topology (smaller c-value = 1.6), featuring relatively smaller link lengths.

The schematic in Figure 4c illustrates the quantification of the *rate of aggregation* using the slope of the hydrograph between the time to achieve minimal dynamic connectivity ($T_{DC_{\min}}$) and maximal dynamic connectivity ($T_{DC_{\max}}$). We define two slopes: $S_{DC_{\min}}$, representing the rate of aggregation from the start of flux propagation from sources until attaining $DC_{\min}$; and $S_{DC_{\max}}$ describing the rate of flux aggregation between the times when $DC_{\min}$ and $DC_{\max}$ are achieved. Since rainfall here is assumed to be spatially uniform and lasting until $T_{DC_{\max}}$, the time to peak discharge occurs at $T_{DC_{\max}}$, with peak discharge being the total number of nodes in the network contributing to the outlet.

Figures 4d and 4e show the calculated $T_{DC_{\min}}$, $T_{DC_{\max}}$, and ΔT, along with the corresponding rates of aggregation as a function of time for the two representative basins shown in Figures 4a and 4b. Since both networks have similar main-channel length, their $T_{DC_{\max}}$ values are comparable (~4 km), whereas the $T_{DC_{\min}}$ of the humid basin (778 m) is greater than that of the dry basin (497 m). This difference arises from the longer channel links in the humid basin compared to the dry one, despite the former having greater side-branching. Thus, for $DC_{\min}$, geometry (link lengths) acts as the dominant control rather than topology. Relatively higher values for $T_{DC_{\min}}$ are observed in humid basins compared to dry basins, although the distribution of $T_{DC_{\max}}$ is similar (see Figure 4i and Figure S3 in Supporting Information S1). Minimum flow connectivity plays a crucial role in linking aquatic habitats and supporting the survival of aquatic species (Rodriguez-Iturbe et al., 2009; Roy et al., 2022). In dry climates, maintaining such connectivity can be challenging; however, shorter link lengths reduce $T_{DC_{\min}}$, which may help sustain habitat connectivity even during dry periods.

Although $T_{DC_{\max}}$ is similar for both basins, indicating that maximal dynamic connectivity is achieved at nearly the same time, the rates at which these peaks are achieved (indicated by $S_{DC_{\min}}$ and $S_{DC_{\max}}$) differ depending on the network structure and climate. We quantify the slopes $S_{DC_{\min}}$ and $S_{DC_{\max}}$ from the normalized hydrographs, where discharge is normalized based on the total number of nodes and the time is normalized based on $T_{DC_{\max}}$. For normalized hydrographs, a lower $S_{DC_{\min}}$ and larger $S_{DC_{\max}}$ would represent an overall faster rate of flux accumulation at the outlet, whereas the opposite case would represent a more gradual increase in discharge. Figure 4f shows the normalized hydrographs for the two sample basins shown in Figures 4a and 4b, highlighting that the

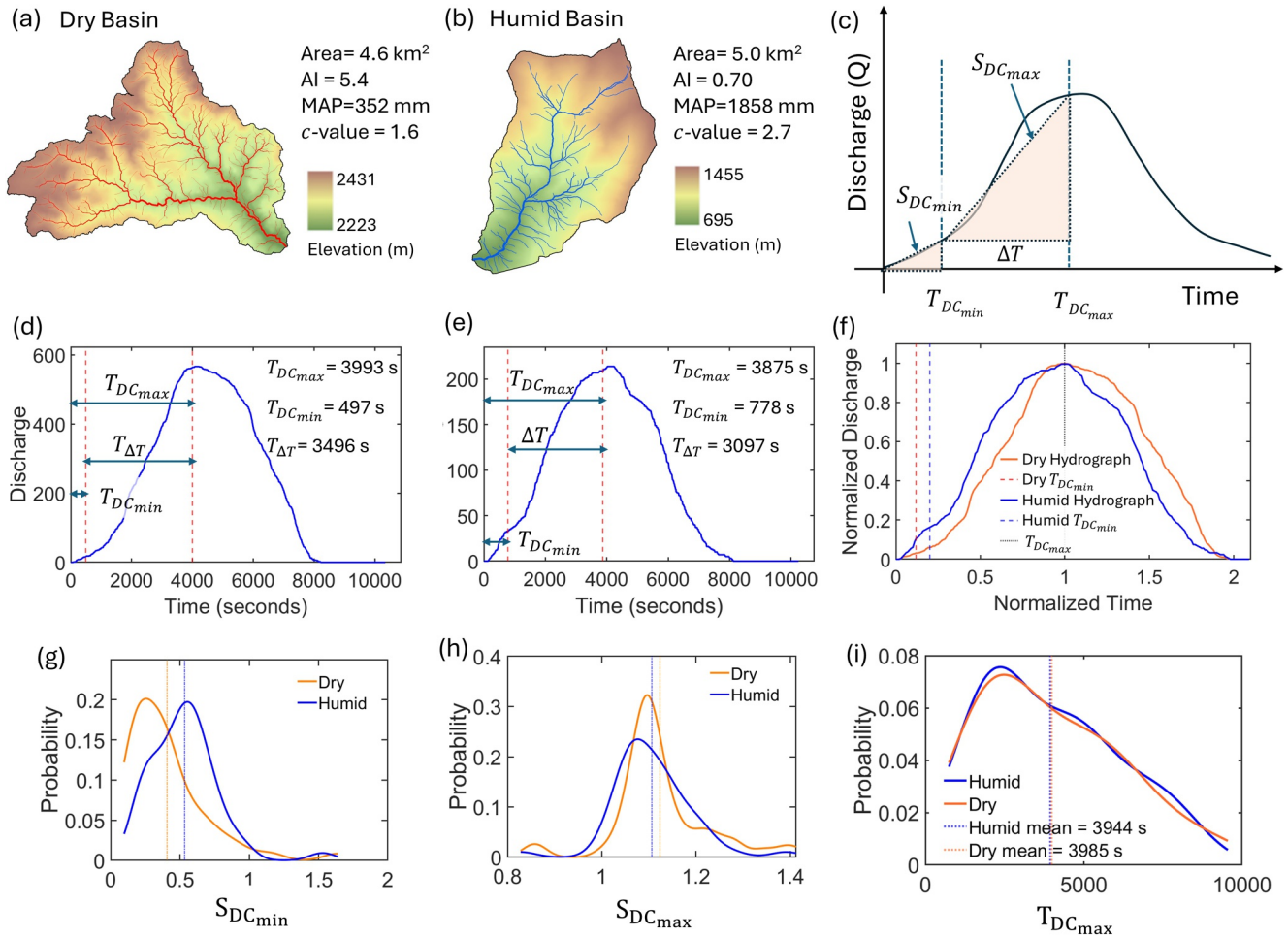

Figure 4. The variation in the rate of aggregation across climatic regimes. Panels (a, b) represent two sample basins with similar drainage area and $T_{DC_{\max}}$ drawn from dry (AI = 5.4) and humid (AI = 0.70) climates, respectively. (c) Schematic for quantification of rate of aggregation (hydrograph) using slope $S_{DC_{\min}}$ and $S_{DC_{\max}}$. (d–e) Hydrographs for the two basins shown in (a) and (b), respectively, highlighting the timing of dynamic connectivity. (f) Normalized hydrographs for the two sample basins. (g–i) Probability distributions (kernel density estimate) of $S_{DC_{\min}}$, $S_{DC_{\max}}$ and $T_{DC_{\max}}$, respectively, calculated for 50 dry and 50 humid basins. This highlights differences in slope values despite the fact that both dry and humid basins have nearly similar $T_{DC_{\max}}$ distribution. Vertical dashed lines in (g–i) represent the mean.

humid basin exhibits a larger $S_{DC_{\min}}$ and a smaller $S_{DC_{\max}}$ than the dry basin, indicative of a slower rate of flux aggregation and a more gradual rise toward peak discharge. This pattern arises from stronger side-branching, which distributes fluxes over longer pathways and delays their convergence. In contrast, the dry basin, which has more branching and less geometric organization (i.e., hierarchy), shows slightly smaller $S_{DC_{\min}}$ and steeper $S_{DC_{\max}}$, implying relatively faster flux aggregation.

The probability distributions of $S_{DC_{\min}}$ and $S_{DC_{\max}}$ computed for all 100 natural basins are shown in Figures 4g and 4h respectively, indicating that, on average humid basins have higher $S_{DC_{\min}}$ reflecting the higher $T_{DC_{\min}}$ in humid basins (see also Figure S3 in Supporting Information S1), and smaller $S_{DC_{\max}}$ highlighting their slower but more buffered hydrologic response compared to dry networks. The faster increase in flux accumulation can also be associated with the tendency for flash floods, which are more common in arid and semi-arid regions. Therefore, the more branched geometry of channel link lengths may contribute to this enhanced flash-flooding behavior. The above results demonstrate that topology dictates the overall shape and timing of the flux aggregation curve, while geometry primarily influences the rate at which initial minimal flow connectivity is achieved. These findings collectively highlight that the interplay between topology and geometry governs not only the timing but also the efficiency of dynamic connectivity, setting the foundation for understanding how climatic factors influence real-world basin responses, as climate has distinct signatures on the topology and geometry of natural networks. We

note that the present dynamic connectivity framework can be further extended to incorporate other important factors, including variations in channel width and depth, channel bed slope, spatio-temporal variability in stream flow velocities, and heterogeneous rainfall patterns. Additionally, the analysis presented here focuses on relatively small basins, and extending it to large basins (e.g., Mississippi River Basin) could provide further insights into the hierarchical behavior of link lengths across varying hydro-climatological, geological, and environmental regimes.

4. Summary and Concluding Remarks

We examined how river network topology and geometry jointly govern the evolution of dynamic connectivity—the process by which fluxes progressively link and aggregate as they move downstream. Extending the dynamic cluster framework of Roy et al. (2022), we incorporated geometric variability of link lengths to distinguish between the onset of minimal dynamic connectivity ($T_{DC_{\min}}$) and the attainment of maximal dynamic connectivity ($T_{DC_{\max}}$).

Our results show that link lengths are hierarchically distributed with stream order, and this geometric hierarchy primarily controls the time to minimal flow connectivity. In contrast, network topology, especially the degree of side-branching, governs the duration between minimal and maximal flow connectivity (ΔT). Randomized-link experiments confirm that removing link-length hierarchy eliminates basin-to-basin variability in ΔT, isolating geometric effects.

Analysis of 100 natural basins across climatic zones further supports these findings: humid basins, with a stronger link-length hierarchy and greater side-branching, exhibit delayed minimal flow connectivity and slower flux aggregation compared to dry basins. Together, these results demonstrate that dynamic connectivity arises from the coupled influence of network topology and geometry, offering a mechanistic explanation for how climate and drainage structure jointly modulate flood timing and flux transport.

Overall, the dynamic connectivity framework presented here provides a quantitative and physically intuitive way to understand how fluxes propagate through branching systems. By explicitly separating the effects of topology and geometry, this approach offers practical guidance for both interpreting natural landscape organization and designing engineered drainage systems. For instance, in new or restored landscapes, the desired hydrologic response—whether rapid drainage or delayed connectivity—can be achieved by tuning the network's branching configuration and link-length hierarchy. Networks with stronger side-branching and a stronger link length hierarchy in stream orders can be used to slow down and delay flux aggregation, which is desirable in urban stormwater systems or flood-prone catchments. Conversely, more branched topologies with a milder link length hierarchy would promote rapid connectivity and efficient transport, suitable for agricultural or engineered systems requiring faster drainage. Beyond hydrology, this framework can also inform ecological and geomorphic design by linking spatial network properties to the timing and rate of connectivity, thus offering a unified tool for analyzing and optimizing both natural and artificial transport networks.

Conflict of Interest

The authors declare no conflicts of interest relevant to this study.

Availability Statement

The DEM data for the natural catchments were obtained from the USGS, and the data of processed DEMs and stream networks is available at Borse et al. (2026).

Acknowledgments

The authors acknowledge support by the National Science Foundation (NSF) Hydrology & Geomorphology and Land-use Dynamics Programs (Grants EAR-2342936; EAR-2342937), the NSF Collaboration in AI and Geosciences (RISE: 2425748), and the NSF Division of Information and Intelligent Systems (Grant IIS2324008). A.S. acknowledges the support from the Preeminent Postdoctoral Program (P3) for D.B. at the University of Central Florida and E.F.-G acknowledges the support by the Samueli Endowed chair at the University of California Irvine. A.T. acknowledges partial support by Ministerio de Ciencia, Innovación y Universidades, Agencia Española de Investigación (MICIU/AEI/-10.13039/501100011033), Grant PID2023-149409NB-I00. Article processing charges were provided in part by the UCF College of Graduate Studies Open Access Publishing Fund. The authors also thank the Editor and the two anonymous reviewers whose suggestions and constructive comments substantially improved our presentation and refined our interpretations.

References

Bavojdan, A. H., Ranjbar, S., Wang, D., & Singh, A. (2025). Signatures of varying climate on geomorphic and topologic characteristics of channel networks. *Water Resources Research*, *61*(4), e2024WR038760. https://doi.org/10.1029/2024WR038760

Benda, L., Poff, N. L., Miller, D., Dunne, T., Reeves, G., Pess, G., & Pollock, M. (2004). The network dynamics hypothesis: How channel networks structure riverine habitats. *BioScience*, *54*(5), 413–427. https://doi.org/10.1641/0006-3568(2004)054[0413:TNDHHC]2.0.CO;2

Borse, D., Roy, J., & Singh, A. (2026). DEMs and stream networks of 100 natural catchments across humid and arid regions of the United States (Version v2) [Dataset]. *Zenodo*. https://doi.org/10.5281/zenodo.19472144

Botter, G., Bertuzzo, E., & Rinaldo, A. (2011). Catchment residence and travel time distributions: The master equation. *Geophysical Research Letters*, *38*(11). https://doi.org/10.1029/2011GL047666

Botter, G., Vingiani, F., Senatore, A., Jensen, C., Weiler, M., McGuire, K. J., et al. (2021). Hierarchical climate-driven dynamics of the active channel length in temporary streams. *Scientific Reports*, *11*(1), 21503. https://doi.org/10.1038/s41598-021-00922-2

Bracken, L. J., & Croke, J. (2007). The concept of hydrological connectivity and its contribution to understanding runoff-dominated geomorphic systems. *Hydrological Processes: International Journal*, *21*(13), 1749–1763. https://doi.org/10.1002/hyp.6313

Carrara, F., Altermatt, F., Rodriguez-Iturbe, I., & Rinaldo, A. (2012). Dendritic connectivity controls biodiversity patterns in experimental metacommunities. *Proceedings of the National Academy of Sciences*, *109*(15), 5761–5766. https://doi.org/10.1073/pnas.1119651109

Carrara, F., Rinaldo, A., Giometto, A., & Altermatt, F. (2014). Complex interaction of dendritic connectivity and hierarchical patch size on biodiversity in river-like landscapes. *The American Naturalist*, *183*(1), 13–25. https://doi.org/10.1086/674009

Carraro, L., Bertuzzo, E., Fronhofer, E. A., Furrer, R., Gounand, I., Rinaldo, A., & Altermatt, F. (2020). Generation and application of river network analogues for use in ecology and evolution. *Ecology and Evolution*, *10*(14), 7537–7550. https://doi.org/10.1002/ece3.6479

Coffey, T. S., & Shaw, J. B. (2017). Congruent bifurcation angles in river delta and tributary channel networks. *Geophysical Research Letters*, *44*(22), 11–427. https://doi.org/10.1002/2017GL074873

Cushman, S. A., & McGarigal, K. (2002). Hierarchical, multi-scale decomposition of species-environment relationships. *Landscape Ecology*, *17*(7), 637–646. https://doi.org/10.1023/A:1021571603605

Czuba, J. A., & Foufoula-Georgiou, E. (2014). A network-based framework for identifying potential synchronizations and amplifications of sediment delivery in river basins. *Water Resources Research*, *50*(5), 3826–3851. https://doi.org/10.1002/2013WR014227

Dodds, P. S., & Rothman, D. H. (2000). Geometry of river networks. II. Distributions of component size and number. *Physical Review E*, *63*(1), 016116. https://doi.org/10.1103/PhysRevE.63.016116

Duquesne, T., & Winkel, M. (2019). Hereditary tree growth and Lévy forests. *Stochastic Processes and their Applications*, *129*(10), 3690–3747. https://doi.org/10.1016/j.spa.2018.10.007

Garbin, S., Celegon, E. A., Fanton, P., & Botter, G. (2019). Hydrological controls on river network connectivity. *Royal Society Open Science*, *6*(2), 181428. https://doi.org/10.1098/rsos.181428

Ghotbi, S., Wang, D., Singh, A., Mayo, T., & Sivapalan, M. (2020). Climate and landscape controls of regional patterns of flow duration curves across the continental United States: Statistical approach. *Water Resources Research*, *56*(11), e2020WR028041. https://doi.org/10.1029/2020WR028041

Gupta, V. K., Waymire, E., & Wang, C. T. (1980). A representation of an instantaneous unit hydrograph from geomorphology. *Water Resources Research*, *16*(5), 855–862. https://doi.org/10.1029/WR016i005p00855

Hansen, A., & Singh, A. (2018). High-frequency sensor data reveal across-scale nitrate dynamics in response to hydrology and biogeochemistry in intensively managed agricultural basins. *Journal of Geophysical Research: Biogeosciences*, *123*(7), 2168–2182. https://doi.org/10.1029/2017JG004310

Hooshyar, M., Singh, A., & Wang, D. (2017). Hydrologic controls on junction angle of river networks. *Water Resources Research*, *53*(5), 4073–4083. https://doi.org/10.1002/2016WR020267

Hooshyar, M., Wang, D., Kim, S., Medeiros, S. C., & Hagen, S. C. (2016). Valley and channel networks extraction based on local topographic curvature and k-means clustering of contours. *Water Resources Research*, *52*(10), 8081–8102. https://doi.org/10.1002/2015WR018479

Horton, R. E. (1945). Erosional development of streams and their drainage basins; hydrophysical approach to quantitative morphology. *Geological Society of America Bulletin*, *56*(3), 275–370. https://doi.org/10.1130/0016-7606(1945)56[275:EDOSAT]2.0.CO;2

Kiffney, P. M., Greene, C. M., Hall, J. E., & Davies, J. R. (2006). Tributary streams create spatial discontinuities in habitat, biological productivity, and diversity in Mainstem Rivers. *Canadian Journal of Fisheries and Aquatic Sciences*, *63*(11), 2518–2530. https://doi.org/10.1139/f06-138

Kirkby, M. J. (1976). Tests of the random network model, and its application to basin hydrology. *Earth Surface Processes*, *1*(3), 197–212. https://doi.org/10.1002/esp.3290010302

Kovchegov, Y., Xu, G., & Zaliapin, I. (2023). Invariant Galton–Watson trees: Metric properties and attraction with respect to generalized dynamical pruning. *Advances in Applied Probability*, *55*(2), 643–671. https://doi.org/10.1017/apr.2022.39

Kovchegov, Y., Zaliapin, I., & Foufoula-Georgiou, E. (2022a). Critical Tokunaga model for river networks. *Physical Review E*, *105*(1), 014301. https://doi.org/10.1103/PhysRevE.105.014301

Kovchegov, Y., Zaliapin, I., & Foufoula-Georgiou, E. (2022b). Random self-similar trees: Emergence of scaling laws. *Surveys in Geophysics*, *43*(2), 353–421. https://doi.org/10.1007/s10712-021-09682-0

Larsen, L. G., Choi, J., Nungesser, M. K., & Harvey, J. W. (2012). Directional connectivity in hydrology and ecology. *Ecological Applications*, *22*(8), 2204–2220. https://doi.org/10.1890/11-1948.1

Muneepeerakul, R., Bertuzzo, E., Rinaldo, A., & Rodriguez-Iturbe, I. (2008). Patterns of vegetation biodiversity: The roles of dispersal directionality and river network structure. *Journal of Theoretical Biology*, *252*(2), 221–229. https://doi.org/10.1016/j.jtbi.2008.02.001

Passalacqua, P., Do Trung, T., Foufoula-Georgiou, E., Sapiro, G., & Dietrich, W. E. (2010). A geometric framework for channel network extraction from lidar: Nonlinear diffusion and geodesic paths. *Journal of Geophysical Research*, *115*(F1). https://doi.org/10.1029/2009JF001254

Peckham, S. D. (1995). New results for self-similar trees with applications to river networks. *Water Resources Research*, *31*(4), 1023–1029. https://doi.org/10.1029/94WR03155

Ranjbar, S., Hooshyar, M., Singh, A., & Wang, D. (2018). Quantifying climatic controls on river network branching structure across scales. *Water Resources Research*, *54*(10), 7347–7360. https://doi.org/10.1029/2018WR022853

Ranjbar, S., Singh, A., & Wang, D. (2020). Controls of the topological connectivity on the structural and functional complexity of river networks. *Geophysical Research Letters*, *47*(22), e2020GL087737. https://doi.org/10.1029/2020GL087737

Rinaldo, A., Gatto, M., & Rodríguez-Iturbe, I. (2020). *River networks as ecological corridors: Species, populations, pathogens*. Cambridge University Press.

Rodriguez-Iturbe, I., Muneepeerakul, R., Bertuzzo, E., Levin, S. A., & Rinaldo, A. (2009). River networks as ecological corridors: A complex systems perspective for integrating hydrologic, geomorphologic, and ecologic dynamics. *Water Resources Research*, *45*(1), W01413. https://doi.org/10.1029/2008WR007124

Rodriguez-Iturbe, I., & Rinaldo, A. (1997). *Fractal river basins: Chance and self-organization*. Cambridge University Press.

Rodríguez-Iturbe, I., & Valdés, J. B. (1979). The geomorphologic structure of hydrologic response. *Water Resources Research*, *15*(6), 1409–1420. https://doi.org/10.1029/WR015i006p01409

Roy, J., Tejedor, A., & Singh, A. (2022). Dynamic clusters to infer topologic controls on environmental transport of river networks. *Geophysical Research Letters*, *49*(6), 1–11. https://doi.org/10.1029/2021GL096957

Sarker, S., Singh, A., Veremyev, A., Boginski, V., & Peckham, S. (2025). Controllability and heterogeneity of river networks using spectral graph theory approach. *Scientific Reports*, *15*(1), 13196. https://doi.org/10.1038/s41598-025-94886-2

Sarker, S., Veremyev, A., Boginski, V., & Singh, A. (2019). Critical nodes in river networks. *Scientific Reports*, *9*(1), 1–11. https://doi.org/10.1038/s41598-019-47292-4

Sassolas-Serrayet, T., Cattin, R., & Ferry, M. (2018). The shape of watersheds. *Nature Communications*, *9*(1), 1–8. https://doi.org/10.1038/s41467-018-06210-4

Schumm, S. A. (1956). Evolution of drainage systems and slopes in badlands at Perth Amboy, New Jersey. *Geological Society of America Bulletin*, *67*(5), 597–646. https://doi.org/10.1130/0016-7606(1956)67[597:EODSAS]2.0.CO;2

Seybold, H., Rothman, D. H., & Kirchner, J. W. (2017). Climate's watermark in the geometry of stream networks. *Geophysical Research Letters*, *44*(5), 2272–2280. https://doi.org/10.1002/2016GL072089

Shao, X., Fang, Y., Jawitz, J. W., Yan, J., & Cui, B. (2019). River network connectivity and fish diversity. *Science of the Total Environment*, *689*, 21–30. https://doi.org/10.1016/j.scitotenv.2019.06.340

Strahler, A. N. (1957). Quantitative analysis of watershed geomorphology. *EOS Transactions of the American Geophysical Union*, *38*(6), 913–920. https://doi.org/10.1029/TR038i006p00913

Tejedor, A., Longjas, A., Zaliapin, I., & Foufoula-Georgiou, E. (2015). Delta channel networks: 1. A graph-theoretic approach for studying connectivity and steady state transport on deltaic surfaces. *Water Resources Research*, *51*(6), 3998–4018. https://doi.org/10.1002/2014WR016577

Tokunaga, E. (1978). *Consideration on the composition of drainage networks and their evolution* (pp. 1–27). Geographical reports of Tokyo Metropolitan University. Retrieved from https://api.semanticscholar.org/CorpusID:126569050

Troutman, B. M., & Karlinger, M. R. (1985). Unit hydrograph approximations assuming linear flow through topologically random channel networks. *Water Resources Research*, *21*(5), 743–754. https://doi.org/10.1029/WR021i005p00743

Wieczorek, M. E., & Signell, R. P. (2023). 30-year (1990-2019) annual average of DAYMET precipitation and temperature for North America [data release]. *U.S. Geological Survey*. https://doi.org/10.5066/P9E0JZ82

Wohl, E., Brierley, G., Cadol, D., Coulthard, T. J., Covino, T., Fryirs, K. A., et al. (2019). Connectivity as an emergent property of geomorphic systems. *Earth Surface Processes and Landforms*, *44*(1), 4–26. https://doi.org/10.1002/esp.4434

Yang, M. S., & Lee, K. T. (2001). Determination of probability distributions for Strahler stream lengths based on Poisson process and DEM. *Hydrological Sciences Journal*, *46*(5), 813–824. https://doi.org/10.1080/02626660109492872

Zaliapin, I., Foufoula-Georgiou, E., & Ghil, M. (2010). Transport on river networks: A dynamic tree approach. *Journal of Geophysical Research*, *115*(F2). https://doi.org/10.1029/2009JF001281

Zanardo, S., Zaliapin, I., & Foufoula-Georgiou, E. (2013). Are American Rivers Tokunaga self-similar? New results on fluvial network topology and its climatic dependence. *Journal of Geophysical Research: Earth Surface*, *118*(1), 166–183. https://doi.org/10.1029/2012JF002392

Zomer, R. J., Xu, J., & Trabucco, A. (2022). Version 3 of the global aridity index and potential evapotranspiration database. *Scientific Data*, *9*(1), 409. https://doi.org/10.1038/s41597-022-01493-1